

# Metal-Insulator-Like Behavior in Semimetallic Bismuth and Graphite

Xu Du, Shan-Wen Tsai[\*], Dmitrii L. Maslov, and Arthur F. Hebard

*Department of Physics, University of Florida, P. O. Box 118440, Gainesville, FL 32611-8440*

(Dated: October 23, 2018)

When high quality bismuth or graphite crystals are placed in a magnetic field directed along the  $c$ -axis (trigonal axis for bismuth) and the temperature is lowered, the resistance increases as it does in an insulator but then saturates. We show that the combination of unusual features specific to semimetals, i.e., low carrier density, small effective mass, high purity, and an equal number of electrons and holes (compensation), gives rise to a unique ordering and spacing of three characteristic energy scales, which not only is specific to semimetals but which concomitantly provides a wide window for the observation of apparent field induced metal-insulator behavior. Using magnetotransport and Hall measurements, the details of this unusual behavior are captured with a conventional multi-band model, thus confirming the occupation by semimetals of a unique niche between conventional metals and semiconductors.

PACS numbers: 71.30.+h, 72.20.My, 71.27.+a, 73.43.Qt

Elemental semimetals, such as bismuth and graphite, are intriguing materials to study because of their high magnetoresistance, low carrier density  $n$ , and high purity. Due to small values of  $n$ , magnetic fields on the order of 10 T are sufficient to drive these semimetals into the ultraquantum regime, where only the lowest Landau level remains occupied. In addition, light cyclotron masses,  $m^*$ , for any field orientation in Bi and along the  $c$ -axis in graphite, result in higher cyclotron frequencies,  $\omega_c = eB/m^*$ , which ensure that quantum magneto-oscillations can be observed at moderate temperatures. High purity facilitates the observation of well-resolved oscillation patterns. These features have made bismuth and graphite perhaps the two most popular materials for studies of quantum magnetic-field effects [1, 2].

Recently, interest in magnetotransport in graphite has been renewed due to observations (similar to those shown in Fig. 1) of an effect that looks like a magnetic-field-induced metal-insulator transition [3, 4]. The metallic  $T$ -dependence of the in-plane resistivity in zero field turns into an insulating-like one when a magnetic field on the order of 10 mT is applied normal to the basal (ab) plane. Increasing the field to about 1 T produces a re-entrance of the metallic behavior [5]. It has been proposed that the low-field effect is due to a magnetic-field-induced excitonic insulator transition of Dirac fermions [5, 6], whereas the high-field one is a manifestation of field-induced superconductivity [5]. It has been also suggested [5] that the apparent metal-insulator transition in graphite is similar to that in 2D heterostructures [7] (although the latter is driven by a field parallel to the conducting plane).

Similar metal-insulating like behavior is also observed in 99.9995% pure bulk bismuth crystals as shown in Fig. 2, where the resistivity is plotted as a function of temperature in successively higher magnetic fields. The crossover from “metallic” to “insulating” behavior has the same qualitative behavior in both semimetals. On lowering the temperature the resistance increases, as it

does in a insulator, but then saturates towards field-dependent constant values at the lowest temperatures. These similarities invite an interpretation that ascribes this interesting behavior to properties shared by both graphite and bismuth, namely low carrier density, high purity, and an equal number of electrons and holes (compensation), rather than to specific properties of graphite: almost 2D nature of transport and a Dirac-like spectrum, as suggested in Refs.[3, 4, 5, 6].

In this letter we demonstrate this connection by examining the magnitude and ordering of three characteristic energy scales: namely, the width of the energy levels  $\hbar/\tau$  where  $\tau$  is the electron-phonon scattering time, the cyclotron energy  $\hbar\omega_c$ , and the thermal energy  $k_B T$ . We provide theoretical justification for, and experimental confirmation of, the existence of a wide interval of temperatures and magnetic fields, defined by the condition,

$$\hbar/\tau \lesssim \hbar\omega_c \lesssim k_B T. \quad (1)$$

In this interval, (a) the magnetoresistance is large, (b) the scattering rate is linear in  $T$ , and (c) Shubnikov de Haas (SdH) oscillations are not resolved due to the thermal smearing of Landau levels. We argue that the unusual behavior of bismuth and graphite is due to the existence of a region, specified by the inequalities of Eq. (1), and also due to compensation between electron and hole charge carriers. Our experimental confirmation is centered on a detailed study of graphite in which we use the conventional theory of multi-band magnetotransport [8] to extract the field-independent carrier density,  $n(T)$ , and scattering time,  $\tau(T)$ , from simultaneous fitting of the temperature and field-dependent longitudinal resistivity  $\rho_{xx}(T, B)$  (magnetoresistance) and transverse resistivity  $\rho_{xy}(T, B)$  (Hall effect). We then show from this analysis that the inequality (1), which is unique to semimetals, is satisfied over a broad temperature and field range.

To illustrate the uniqueness of low-carrier-density semimetals, we compare them with conventional, high-density, uncompensated metals. To begin with, if the

Fermi surface is isotropic, a metal exhibits no magnetoresistance because the Lorentz force does not have a component along the electric current [8]. In anisotropic metals the magnetoresistance is finite and proportional to  $(\omega_c\tau)^2$  in weak magnetic fields, i.e., for  $\omega_c\tau \ll 1$ . In stronger fields ( $\omega_c\tau \gg 1$ ), classical magnetoresistance saturates, if the Fermi surface is closed [9]. In contrast, transverse magnetoresistance of a semimetal grows as  $B^2$  both in the weak- and strong-field regimes [9].

The magnetoresistance  $[\rho(B) - \rho(0)]/\rho(0)$  is much larger in semimetals than in conventional metals. In addition to the saturation effect, described above, another important factor that limits the magnetoresistance in conventional metals is the higher scattering rates and thus smaller values of the  $\omega_c\tau$  product. The impurity scattering rate in semimetals is smaller than in conventional metals simply because semimetals are typically much cleaner materials. The lower carrier density of semimetals also reduces the rates of electron-phonon scattering in semimetals compared to that of conventional metals. For temperatures above the transport Debye temperature, which separates the regions of the  $T$ - and  $T^5$ -laws in the resistivity,  $\Theta_D^\rho = 2\hbar k_F s/k_B$ , where  $k_F$  is the Fermi wavevector and  $s$  is the speed of sound (both properly averaged over the Fermi surface), one can estimate the electron-phonon scattering rate as  $\tau^{-1} \simeq (k_F a_0)(m^*/m_0)k_B T/\hbar$ , where  $a_0$  is the atomic lattice constant, and  $m^*$  and  $m_0$  are respectively the effective and bare electron masses [10]. In a conventional metal,  $k_F a_0 \simeq 1$  and  $m^* \simeq m_0$ . In this case,  $\Theta_D^\rho$  is of order of the thermodynamic Debye temperature  $\hbar s/k_B a_0 \simeq \text{few } 100 \text{ K}$  and  $\tau^{-1} \simeq k_B T/\hbar$ . In low-carrier-density materials ( $k_F a_0 \ll 1$ ), which typically also have light carriers ( $m^* \ll m_0$ ),  $\Theta_D^\rho$  is much smaller and thus  $\tau^{-1} \ll k_B T/\hbar$ . Therefore, in a low-carrier-density semimetal there exists a wide interval of temperatures and magnetic fields, defined by the inequalities (1). In contrast, there is no wide interval between  $\hbar/\tau$  and  $k_B T$  in a conventional metal [11].

An additional feature, crucial for interpreting the experimental data, is that the Fermi energies of graphite ( $E_F = 22 \text{ meV}$ ) [12] and bismuth ( $E_F = 30 \text{ meV}$  [holes]) [13] are relatively low and the temperature dependence of the resistivity comes from two temperature-dependent quantities:  $n(T)$  and  $\tau(T)$ . Purity of materials ensures that electron-phonon scattering is a dominant mechanism for resistance over a wide temperature range.

Standard 4-probe measurements were carried out on single-crystal highly oriented pyrolytic graphite (HOPG) sample with a  $2^\circ$  mosaic spread, as determined by X-rays. The resistivity was measured using an ac (17 Hz) resistance bridge over the temperature range 5K-350K. In all the measurements, the magnetic fields were applied perpendicular to the sample basal planes. Both  $\rho_{xx}$  and  $\rho_{xy}$  (Fig. 3) were measured in magnetic fields up to 1 T, although the analysis (solid lines) was limited

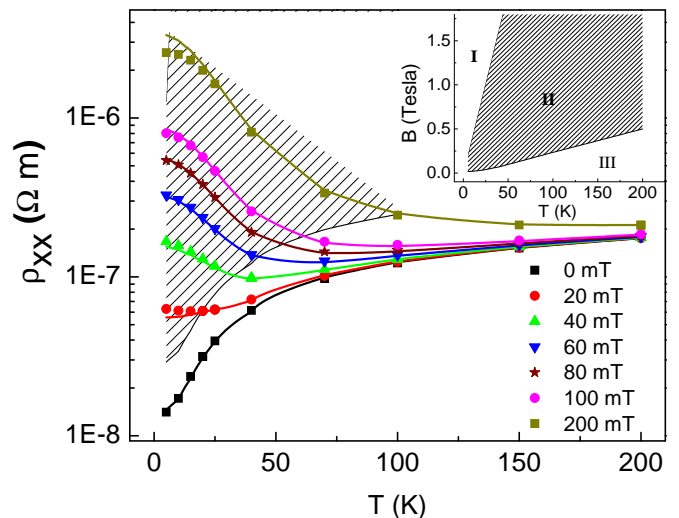


FIG. 1: Temperature dependence of the ab-plane resistivity  $\rho_{xx}$  for a graphite crystal at the c-axis magnetic fields indicated in the legend. The solid lines are the fits to the data using the six parameters derived from the three-band analysis described in the text. The shadowed region in the inset and its mapping onto the data in the main panel indicates the interval defined by Eq.(1).

to  $B \leq 200 \text{ mT}$ . A small field-symmetric component due to misaligned electrodes was subtracted from the  $\rho_{xy}(B)$  data.

We used a standard multi-band model [8] to fit the data. Each band has two parameters: resistivity  $\rho_i$  and Hall coefficient  $R_i = 1/q_i n_i$ , where  $q_i = \pm e$  is the charge of the carrier. In agreement with earlier studies, we fix the number of bands to three [2]. Two of these are the majority electron and hole bands, and the third is the minority hole band [2]. Although the third band is not essential for a qualitative understanding of the data, it is necessary for explaining the low-field fine features in  $\rho_{xy}$  shown in the inset of Fig 3. The minority band makes a negligible contribution at higher fields due to its low carrier concentration.

We fit  $\rho_{xx}$  and  $\rho_{xy}$  simultaneously by adjusting the six parameters independently, until differences between the fitting curves and the experimental data are minimized. Because the majority carriers in graphite derive from Fermi surfaces that have six-fold rotational symmetry about the c-axis, we only need to use the 2x2 magneto-conductivity tensor  $\hat{\sigma}^i$  with elements  $\sigma_{xx}^i = \sigma_{yy}^i = \rho_i / [\rho_i^2 + (R_i B)^2]$  and  $\sigma_{xy}^i = -\sigma_{yx}^i = -R_i B / [\rho_i^2 + (R_i B)^2]$ , where  $\rho_i = m_i^*/n_i e^2 \tau_i$ . The total conductivity,  $\hat{\sigma} = \sum_{i=1}^3 \hat{\sigma}^i$ , is simply a sum of the contributions from all the bands and the total resistance is  $\hat{\rho} = \hat{\sigma}^{-1}$ .

Qualitatively, the unusual temperature dependence

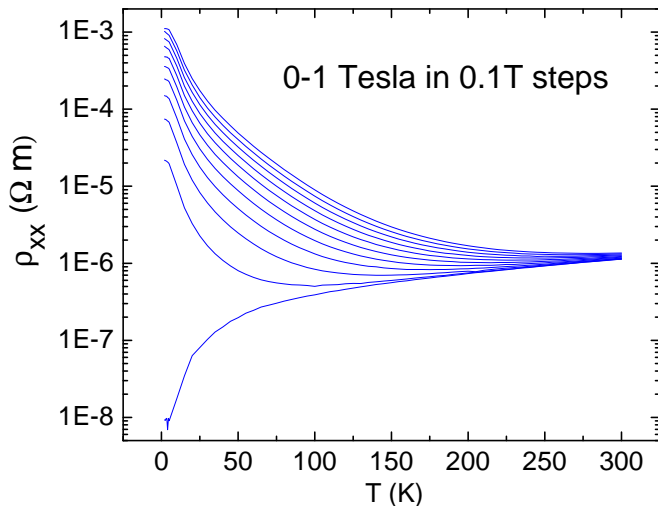


FIG. 2: Temperature dependence of the longitudinal resistivity for a bismuth crystal at magnetic fields ranging from 0 to 1 T in 0.1 T steps from top to bottom. The magnetic field and the current are along the trigonal and binary axes, correspondingly. In zero field, the resistance is approximately linear in temperature.

displayed in Fig. 1 can be understood for a simple two-band case where  $\rho_{xx}$  reduces to

$$\rho_{xx} = \frac{\rho_1 \rho_2 (\rho_1 + \rho_2) + (\rho_1 R_2^2 + \rho_2 R_1^2) B^2}{(\rho_1 + \rho_2)^2 + (R_1 + R_2)^2 B^2}. \quad (2)$$

Assuming that  $\rho_{1,2} \propto T^a$  with  $a > 0$ , we find that for perfect compensation,  $R_1 = -R_2 = |R|$ , Eq. (2) can be decomposed into two contributions: a field-independent term  $\propto T^a$  and a field-dependent term  $\propto R^2(T)B^2/T^a$ . At high  $T$ , the first term dominates and metallic behavior ensues. At low  $T$ ,  $R(T) \propto 1/n(T)$  saturates and the second term dominates, giving “insulating” behavior.

The actual situation is somewhat more complicated due to the  $T$ -dependence of the carrier concentration, the presence of the third band, and imperfect compensation between the majority bands. Results for the temperature-dependent fitting parameters are shown in Fig. 4 where band 1 corresponds to majority holes, band 2 to majority electrons and band 3 to minority holes. The insulating-like behavior of the carrier density with a tendency towards saturation at low temperatures is well reproduced. For the majority bands, 1 and 2, the carrier concentrations are approximately equal and similar in magnitude to literature values [2]. The slope of the linear-in- $T$  part of  $\tau^{-1} = \alpha_{\text{exp}} k_B T / \hbar$  with  $\alpha_{\text{exp}} = 0.065(3)$  (dashed line in Fig. 4, top panel) is consistent with the electron-phonon mechanism of scattering. To see this, we adopt a simple model in which carriers occupying the ellipsoidal Fermi surface with parameters  $m_{ab}$  (equal to  $0.055m_0$  and  $0.040m_0$  for electrons

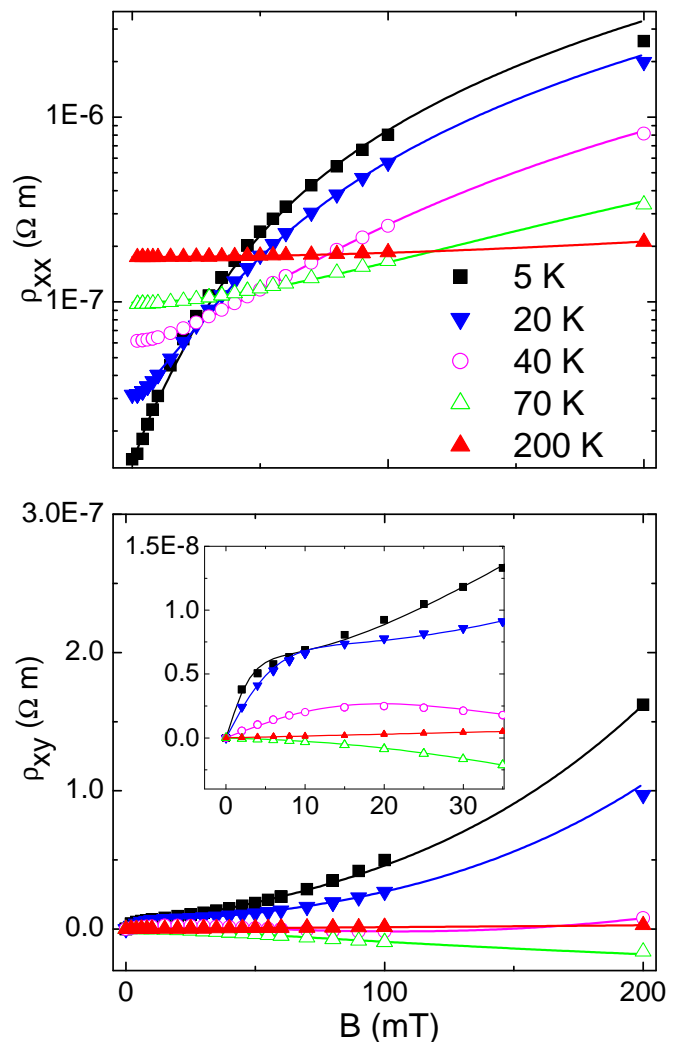


FIG. 3: Longitudinal resistivity  $\rho_{xx}$  (top panel) and transverse resistivity  $\rho_{xy}$  (bottom panel) versus applied field  $B$  for graphite at the temperatures indicated in the legend. The solid lines are determined by a fitting procedure that simultaneously includes both sets of data into a three-band model described in the text. The inset in the bottom panel, with the same units on each axis, magnifies the low-field region, where the contribution from the third band with a lower carrier density makes a major contribution that cannot be fit by solely using the two majority bands.

and majority holes, correspondingly) and  $m_c$  (equal to  $3m_0$  and  $6m_0$ , correspondingly) interact with longitudinal phonons via a deformation potential, characterized by the coupling constant  $D$  (equal to 27.9 eV). In this model, the slope in the linear-in- $T$  dependence of  $\tau^{-1}$  is given by [10]  $\alpha_{\text{theor}} = (\sqrt{2}/\pi) \sqrt{(m^*)^3 E_F D^2 / \rho_0 s_{ab}^2 \hbar^3}$ , where  $m^* = (m_{ab}^2 m_c)^{1/3} \approx 0.21m_0$  both for electrons and holes,  $\rho_0 = 2.27 \text{ g/cm}^3$  is the mass density of graphite, and  $s_{ab} = 2 \times 10^6 \text{ cm/s}$  is the speed of sound in the ab-

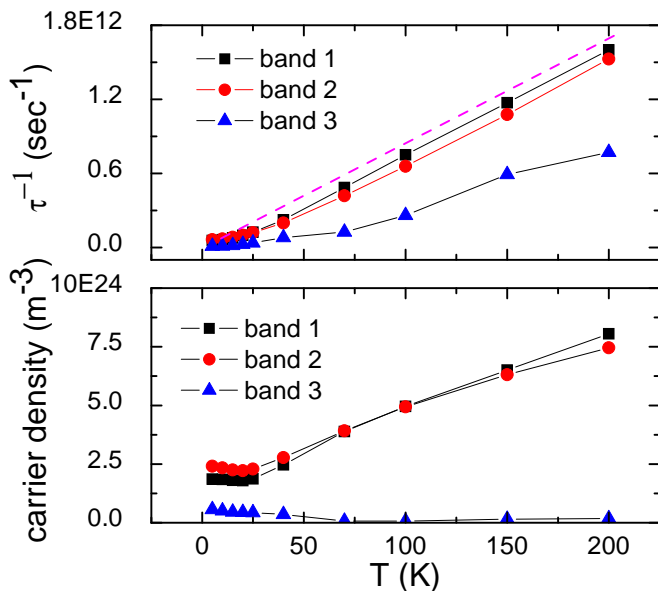


FIG. 4: Temperature dependence of the fitting parameters (graphite) for the bands indicated in the legends of each panel. The near equality of the carrier densities of the two majority bands (lower panel) indicates good compensation at low fields ( $B < 200$  mT) and the linear dependence of the scattering rate on  $T$  (upper panel, dashed line) with a slope of  $0.065(3)$  in units of  $k_B/\hbar$  is consistent (see text) with electron-phonon scattering.

plane. (The numerical values of all parameters are taken from the standard reference on graphite [2].) With the above choice of parameters,  $\alpha_{\text{theor}} = 0.052$  for both types of carriers. This value is within 20% of the value found experimentally. Given the simplicity of the model and the uncertainty in many material parameters, especially in the value of  $D$ , such an agreement between theory and experiment is quite satisfactory.

The solid lines through the data points in Fig. 1 are calculated from the temperature-dependent fitting parameters derived from our three-band analysis and plotted in Fig. 4. The shaded region (II) depicted in the inset of Fig. 1 represents those temperatures and fields that satisfy the inequalities in (1). In region (I) SdH oscillations can be seen at sufficiently low  $T$ . Our sample has a Dingle temperature of 3.0 K. The boundary between (I) and (II) reflects the rightmost inequality of (1) and is determined by the relation  $T > \hbar eB/m^*$ . The boundary between (II) and (III) reflects the leftmost inequality of (1) and is determined by the relation  $B > m^*/e\tau(T)$  where  $1/\tau(T)$  is obtained from experimental fitting parameters (Fig. 4). In the main panel of Fig. 1 we superimpose region (II), again as a shaded area, on the  $\rho_{xx}(T, B)$  data. Below the lower boundary  $\omega_c\tau < 1$ , and the magnetoresistance is relatively small. The upper boundary is determined by the locus of  $(B, T)$  points satisfying the rightmost in-

equality of (1). Clearly region (II), constrained by the inequalities of (1), overlaps well with the metal-insulating like behavior of graphite. Since the majority bands of bismuth comprise three non-coplanar electron ellipsoids and one hole ellipsoid, a similar analysis for bismuth is more complicated and would require more space than available here.

We thus conclude that the semimetals graphite and, by implication, bismuth share the common features of high purity, low carrier density, small effective mass and near perfect compensation and accordingly obey the unique energy scale constraints that allow pronounced metal insulating behavior accompanied by anomalously high magnetoresistance. At magnetic fields higher than discussed in this paper ( $B \geq 1$  T) we believe that the multi-band model is still appropriate and may provide an alternative explanation for the reentrant behavior observed by us and others [5].

Subsequent to the completion of this study, we were informed of recent work [T. Tokumoto *et al.*, Solid State Commun. 129, 599 (2004)] which used a two-band model to explain the unusual behavior of  $\rho_{xx}(T, B)$  in graphite.

This work was supported in part by the National Science Foundation under Grants No. DMR-0101856 (AFH) and DMR-0308377 (DLM) and by the In House Research Program of the National High Magnetic Field Laboratory, which is supported by NSF Cooperative Agreement No. DMR-0084173 and by the State of Florida. SWT and DLM acknowledge the hospitality of the Aspen Center for Theoretical Physics, where part of the analysis was performed. The authors are especially thankful to J. E. Fischer and R. G. Goodrich for supplying respectively the HOPG and Bi samples, J. Derakhshan for assistance with the Bi measurements, and J. S. Brooks for discussions.

- 
- [\*] Department of Physics, Boston University, 590 Commonwealth Ave., Boston, MA 02215.
- [1] V. S. Edel'mann, Sov. Phys. Usp. 20, 819 (1977).
- [2] N. B. Brandt, S. M. Chudinov, and Y. G. Ponomarev, Semimetals 1: Graphite and its compounds (North-Holland, 1988).
- [3] Y. Kopelevich *et al.*, Phys. Solid State 41, 1959 (1999).
- [4] H. Kempa, *et al.*, Solid State Commun. 115, 539 (2000), *ibid.*, 121, 579 (2002).
- [5] Y. Kopelevich *et al.*, Phys. Rev. Lett. 90, 1564021 (2003).
- [6] D. V. Khveshchenko, Phys. Rev. Lett. 87, 206401 (2001).
- [7] E. Abrahams, S. V. Kravchenko, and M. P. Sarachik, Rev. Mod. Phys. 73, 251 (2001).
- [8] N. W. Ashcroft and N. D. Mermin, Solid State Physics (Holt, Rinehart and Winston, 1976).
- [9] A. A. Abrikosov, Fundamentals of the Theory of Metals (North-Holland, 1988).
- [10] V. F. Gantmakher and Y. B. Levinson, Carrier scattering in metals and semiconductors (North-Holland, 1987).

- [11] Inequality Eq.(1) can be satisfied in a typical metal for  $T \ll \Theta_D^p$  when the inverse (transport) time  $\tau_{tr}^{-1} \propto T^5 \ll k_B T / \hbar$ . For an uncompensated metal with a closed Fermi surface, however, magnetoresistance saturates in this regime.
- [12] J. W. McClure and W. J. Spry, Phys. Rev. 165, 809 (1968).
- [13] G. E. Smith, G. A. Baraff, and J. M. Rowell, Phys. Rev. 135, A1118 (1964).
- [14] S. Cho, Y. Kim, A. J. Freeman, et al., App. Phys. Lett. 79, 3651 (2001).
- [15] F. Y. Yang, K. Liu, K. Hong, et al., Science 284, 1335 (1999).